A study of the fracture behaviour of polyethersulphone

P. J. Hine, R. A. Duckett and I. M. Ward
Department of Physics, University of Leeds, Leeds, UK
(*Received* 7 *April* 1981)

The fracture behaviour of polyethersulphone has been studied by combining fracture toughness measurements with optical examination of the craze and shear lips at the tip of the crack. It is shown that the behaviour can be very well described by a mixed mode fracture model in which the total strain energy release rate contains a plane strain term from the craze and a plane stress term from the shear lips. In unannealed samples the craze shape was well approximated by the Dugdale plastic zone model, but this was not so for annealed samples. The effect of annealing on the fracture behaviour is discussed in qualitative terms.

INTRODUCTION

In previous publications[1-3], the fracture behaviour of polycarbonate has been discussed in terms of 'mixed mode' fracture where the central portions of the specimens fail in plane strain in a brittle mode of failure, whereas the edges fail in plane stress in a ductile mode (the so-called shear lips). In this paper we will discuss the fracture behaviour of another glassy polymer, polyethersulphone (PES), where similar features have been observed, and consequently we have adopted a very similar approach to obtain a quantitative analysis.

In polyethersulphone, as in polycarbonate and polymethylmethacrylate, optical examination of the crack tip region shows that there is a clearly resolved craze at the crack tip in the central plane strain region. As in previous publications the approach is to observe the interference fringe pattern produced by the craze, and use this to compare the craze shape with that predicted by the Dugdale zone model[4-7]. In this way it is possible to obtain estimates of the crack opening displacement in the craze, the craze stress and the plane strain fracture toughness.

The craze shape measurements are combined with direct measurements of the overall fracture toughness by compact tension fracture measurements, in a range of samples of different thickness and different shear lip widths. On the basis that we can assign different critical strain energy release rates to the plane strain and plane stress areas, the total measured strain energy release rate is given by adding their relative contributions, assuming that the plane stress contribution is proportional to the volume of the shear lips. This procedure is different from that proposed by Parvin and Williams[3], where additivity of stress intensity factors is assumed, but has been shown to give very good numerical agreement in the case of polycarbonate. Moreover, as will be shown here for polyethersulphone, the energy dissipated in the shear lips corresponds well with direct measurements of the work to rupture in a thin sheet. The plane strain fracture toughness values found from these direct fracture measurements also agree well with those predicted from the craze shape data.

It has been found that the fracture behaviour of PES is markedly affected by annealing. We have therefore examined the validity of the mixed mode failure model for a range of PES samples prepared by subjecting the polymer to a range of annealing treatments.

EXPERIMENTAL

The materials used in this investigation were 3 and 6 mm plaques of PES injection moulded from polymer supplied by ICI Ltd. Fracture tests were performed using an Instron tensile testing machine, on compact tension specimens machined from these plaques (*Figure 1*).

Three methods for producing a sharp initial starting crack were tried but only one gave stable crack propagation. Initially, following methods successfully used with other polymers, a razor blade was pushed slowly into the sample. This was found to cause a region of plastic deformation around the crack tip which inhibited craze initiation and resulted in 'stick-slip' crack propagation. Subsequent attempts to initiate sharp cracks by fatigue produced similar results. The successful method which involved tapping a razor blade into the sample appeared to propagate a sharp crack through any yielded zone which might have been produced. This method produced stable crack growth on loading which it is believed was independent of the notching procedure, although it would probably not work for a more brittle polymer.

The shapes of crazes formed at the tips of growing cracks were observed using the technique previously described[4]. Portions of the compact tension specimens containing the crack tip were cut out (*Figure 2*), polished on one surface and observed in the direction perpendicular to the crack plane in a conventional incident-light microscope. The crazes were loaded by pushing either a razor blade or a more blunt wedge into the crack. A series of photographs were taken of the constant thickness interference fringes visible within the craze as the load was increased, the last one before crack propagation occurred being taken as an approximation to the moving crack. A microdensitometer was used to analyse the fringe pattern on the resulting negative. The

0032-3861/81/121745-09$02.00

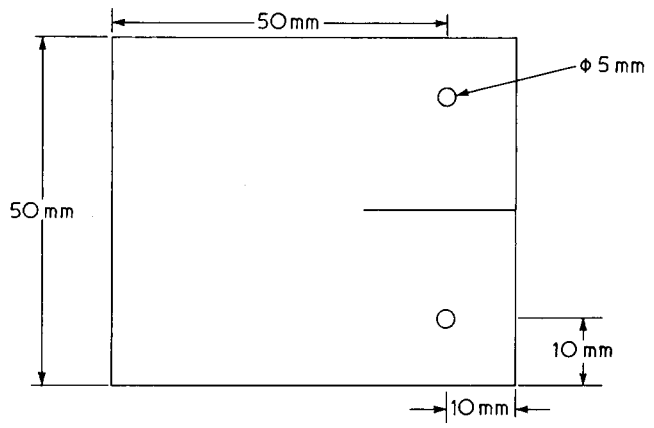

Figure 1 Compact tension specimen geometry

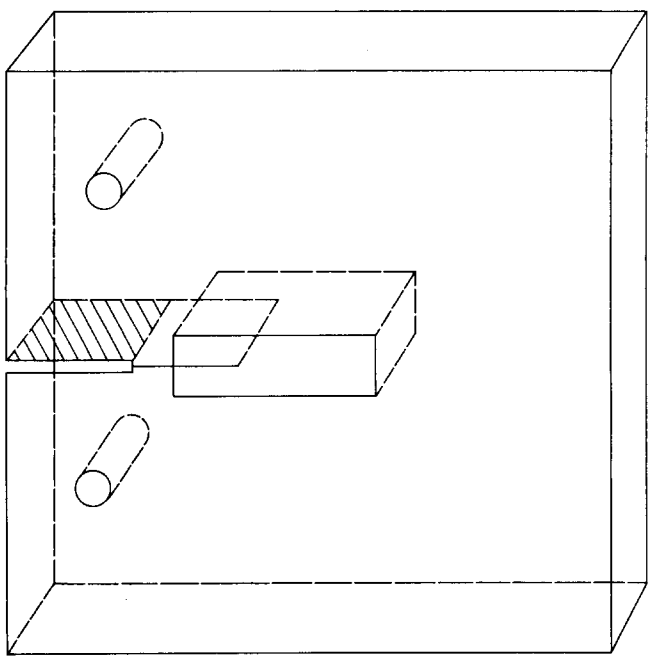

Figure 2 Compact tension specimen showing the portion cut away for viewing of the craze

widths of shear lips where observed on the fracture surface, were measured directly in the optical microscope.

A typical load/displacement plot is shown in *Figure 3* from which it can be seen that the decrease in load P during crack propagation was approximately linear with increase in crosshead displacement Δ; and measurements of crack length indicated that the crack speed was also constant. Under these conditions it can be shown that the strain energy release rate is given by

$$G_c = \frac{-\Delta_f}{2B}\left(\frac{dP}{da}\right)$$

where a is the crack length, B sample thickness and Δ_f is defined in the figure. G_c can therefore be obtained simply from measurements of load P and crack length a as a function of crosshead displacement.

Following previous work a study has been made of whether the craze shape is described by the Dugdale plastic zone model[7]. This model describes the size and shape of a plastic zone ahead of the crack, subject to internal stresses σ_0 such that the stress intensity at the crack tip is reduced to zero, hence removing the stress singularity (*Figure 4*). Rice[8] has shown how the thickness, δ, of the zone at any point distance x_1 from the crack-tip is given by

$$\delta = \frac{8\sigma_0 R}{\pi E^*}\left\{\xi - \frac{x_1}{2R}\log\left(\frac{1+\xi}{1-\xi}\right)\right\} \quad (2)$$

where $\xi = (1 - x_1/R)^{1/2}$, R = plastic zone length, and E^* is the 'reduced' Young's modulus, $E^* = E/(1-\nu^2)$ (ν is Poisson's ratio).

Strictly this model applies for an infinite plate with a centre crack of length $2a$, the plate loaded in tension remote from the crack. In these experiments the craze is observed at the tip of a wedge loaded crack of length a, (*Figure 5*). Rice[9] has indicated how this difference in loading should influence the plastic zone shape. Using his guidelines a modified expression has been developed to model the loading used here.

$$\delta = \frac{8\sigma_0 R}{\pi E^*}\left\{\xi - \frac{x_1}{2R}\log\left(\frac{1+\xi}{1-\xi}\right) + A\log\left(\frac{A+\xi}{A-\xi}\right) - 2\xi\right\} \quad (3)$$

where $A = (1 + a/R)^{2/2}$.

It can be seen that the second 'log' term expands to

$$A\ln\left(\frac{A+\xi}{A-\xi}\right) = 2A\left\{\frac{\xi}{A} + \frac{1}{3}\left(\frac{\xi}{A}\right)^3 + \frac{1}{5}\left(\frac{\xi}{A}\right)^5 + \ldots\right\}$$

and so for a short craze where $R/a \to 0$ and $A \to \infty$, equation (3) reduces to the normal expression (equation (2)).

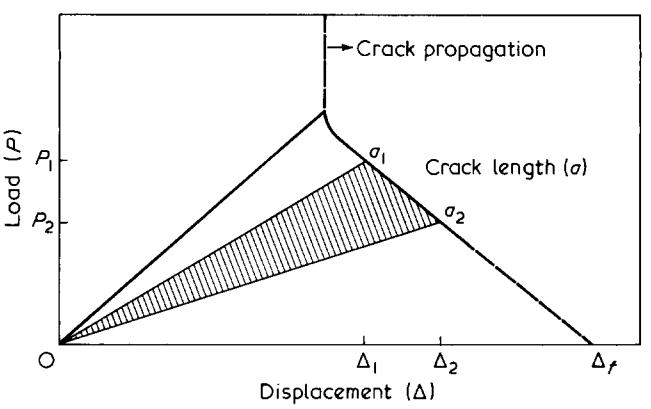

Figure 3 Typical load/displacement plot for crack propagation in a compact tension specimen

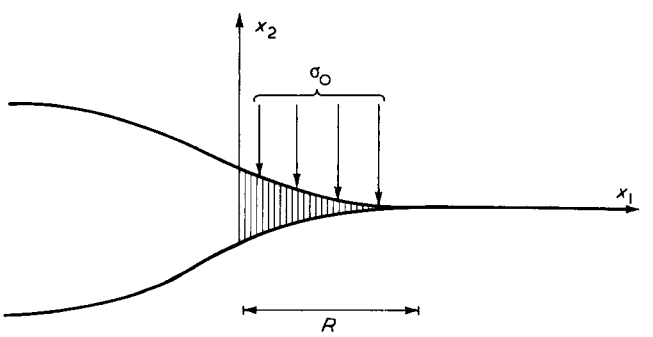

Figure 4 Dugdale plastic zone

In situations where the Dugdale model describes the experimental craze shape the following equations can be used to determine various fracture parameters

$$R=\frac{\pi}{8}\left(\frac{K_c}{\sigma_0}\right)^2 \tag{4}$$

$$G_c=\sigma_0\delta_c \tag{5}$$

where K_c = critical stress intenxity factor = $\sqrt{E^*G_c}$;
δ_c = critical crack opening displacement (*COD*),
and σ = internal stress within the craze (craze stress).

In order to determine these parameters and to understand the fracture mechanisms two series of experiments were performed to measure the modulus E^* and the yield stress σ_y over a range of strain-rates. Four point bend tests were used for measurements of the modulus E and standard dumbell specimens were used for the tensile yield stress. A value of $\nu=0.39$ was used in conjunction with the modulus E to calculate a value for $E^*(=E/(1-\nu^2))$.

Finally, a set of tests were carried out on samples of PES that had been annealed for various periods of time from $\frac{1}{4}$ h to 6 h at 200°C and then cooled slowly in the oven to room temperature. It is believed that this process simulates the likely effects on the craze shape and fracture toughness of prolonged ageing at room temperature.

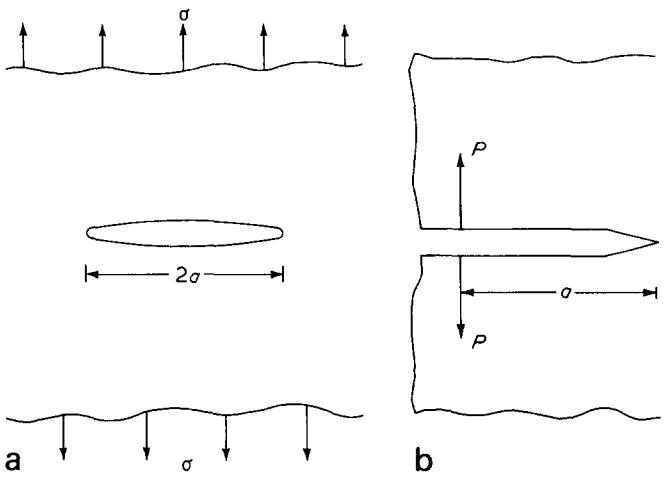

Figure 5 Models of crack geometry and loading, (a) for an infinite plate with remote loading and (b) for an edge crack wedge loaded

RESULTS AND DISCUSSION

Craze shape studies

Examples of the interference patterns produced in untreated PES are shown in *Figures 6a* and *b*. The position of each fringe was measured by traversing a microdensitometer across the photographic negative for each particular sample. Comparison of the data with the Dugdale model (equations (2) and (3)) was made by assuming particular values of R and δ_c then computing the sum of the squares of differences between the measured fringe positions and the model predictions for each fringe. The values of R and δ_c were then varied to minimize this sum, resulting in a 'best fit' to the model.

An example of a craze at the tip of a long crack ($\sim$4 cm) in untreated PES is shown in *Figure 7* and it can be seen that the Dugdale model provides a very good description of the craze shape in this situation. *Figure 8* shows comparison between the observed shape and the Dugdale model for a craze at the tip of a short ($\sim$3 mm) crack. It

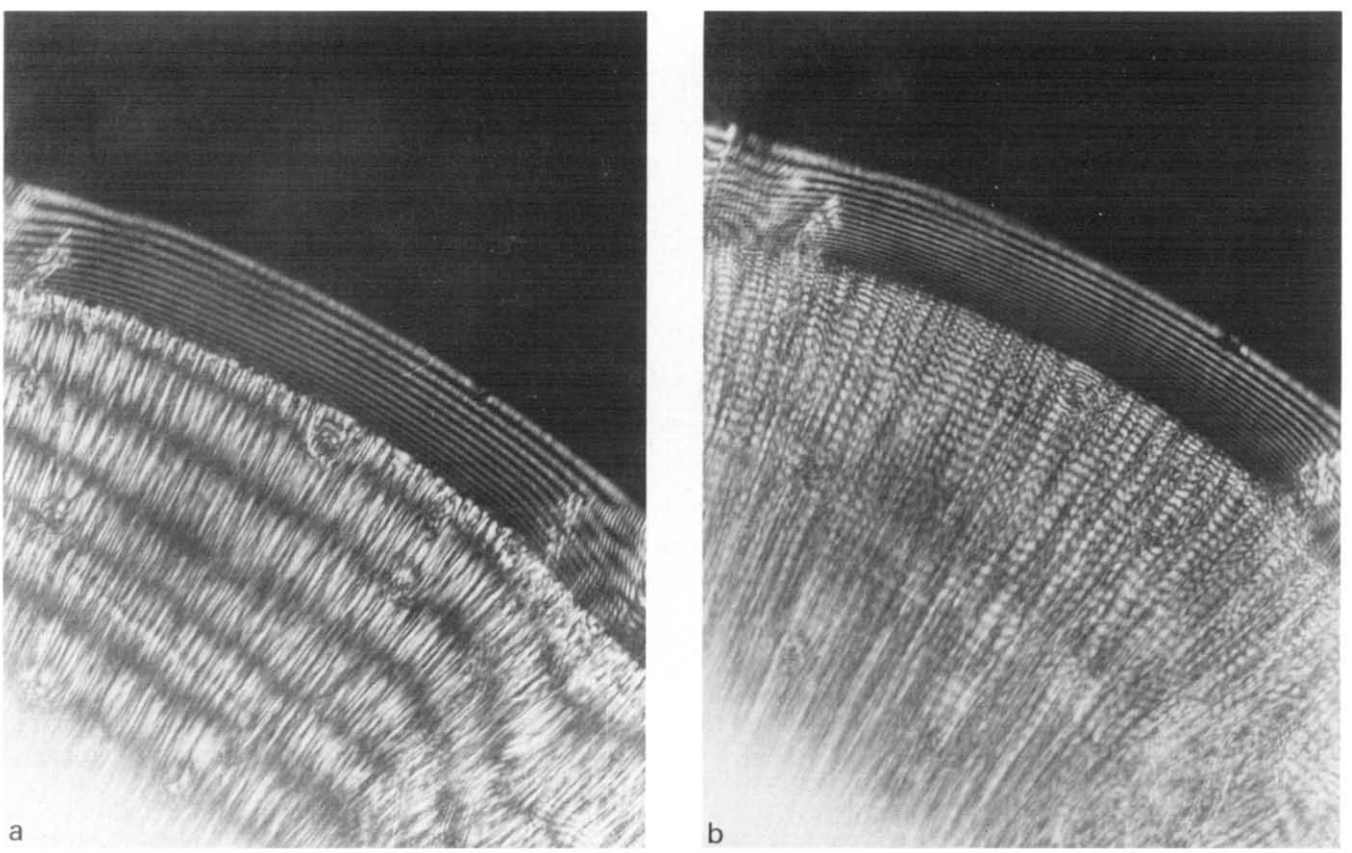

Figure 6 Interference patterns in untreated PES (a) unloaded and (b) loaded

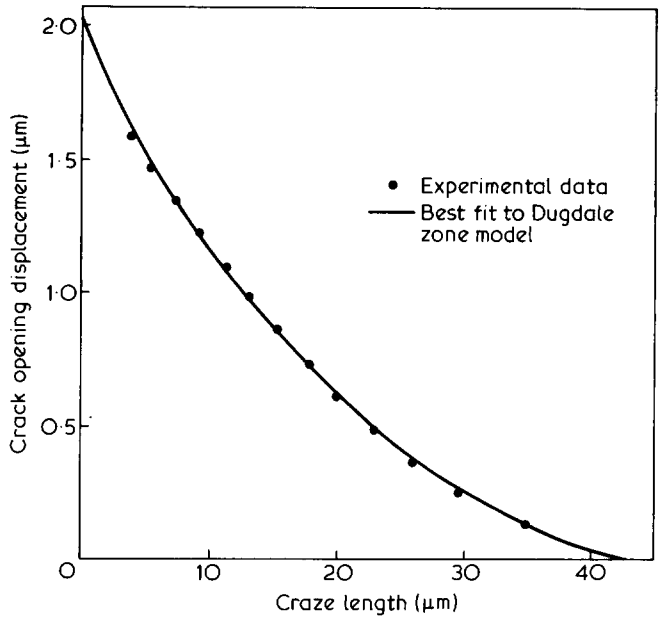

Figure 7 Comparison of experimental data with the Dugdale model for a crack length of ≃4 cm

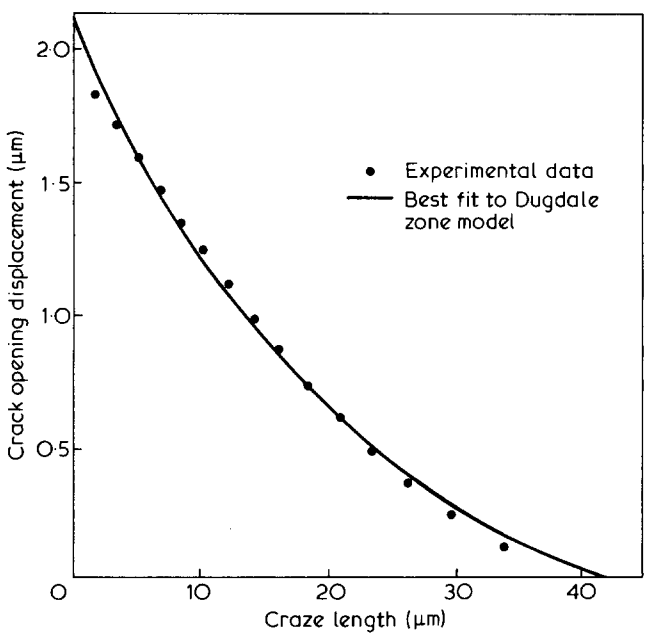

Figure 8 Comparison of experimental data with the Dugdale model for a crack length of ≃3 mm

can be seen that the actual shape has a wedge-shaped profile, with substantially lower curvature than the Dugdale model. Even in this case, with a short crack, there is very little distinction between the predictions of equations (2) and (3) and there are systematic discrepancies between the observed shape and the model. This is confirmed by *Figure 9* which is a plot of the 'root mean square deviation' between observation and model as a function of the crack length. Thus it is concluded that the Dugdale model describes well the observed craze shape ahead of long cracks in untreated PES, but that significant differences in craze shape are observed with short cracks and that these cannot be described by the Dugdale model, even when modified to take into account the crack length.

Following these observations the craze at the tip of a 4 cm crack length was used to determine the various fracture parameters using equations (2), (4) and (5).

From basic interference theory, the thickness $\delta(x_1)$ at a bright fringe is given

$$\delta(x)=(n_x+\tfrac{1}{2})\frac{\lambda'}{2\mu} \tag{6}$$

where $n_x=0, 1, 2 \ldots=$ order of bright fringe at x; λ', wavelength of incident light; μ, refractive index of craze. To determine the absolute value of the critical crack opening displacement $\delta(0)=\delta_c$, a value is required for the refractive index of the craze at break μ_B. This is related to the refractive index of the unloaded craze μ_0 by the relationship[4]

$$\frac{\mu_B\lambda}{\mu_0}=\frac{n_b}{n_0}=1+\frac{(\lambda-1)}{\mu_0} \tag{7}$$

where n_b is number of fringes when loaded; n_0, number of fringes when unloaded; λ, extension ratio of craze.

The value of the refractive index for the craze μ_0 is not available in the literature so an estimate had to be made based on values of the bulk and craze refractive indices for polymethylmethacrylate (PMMA)[10,11] and polycarbonate[12] (PC).

For PMMA Bulk $RI=1.49$

Craze $RI=1.32$

and for PC Bulk $RI=1.59$

Craze $RI=1.27$

These values give ratios of the craze/bulk refractive index of 0.88 for PMMA and 0.80 for PC. Using a bulk refractive index for PES of 1.59, and an 'average' value of craze/bulk refractive index of 0.84, this gives a value of 1.34 for the craze refractive index, μ_0 of PES.

From the best fit to the craze shown in *Figure 6* it was found that $n_0=11$, $n_b=16.6$ and the craze length $R=43.5$ μm. This gave a value for λ of 1.69 and hence a value for μ_B of 1.21. (All observations of the crazes were performed using a mercury lamp and a green filter giving λ' equal to

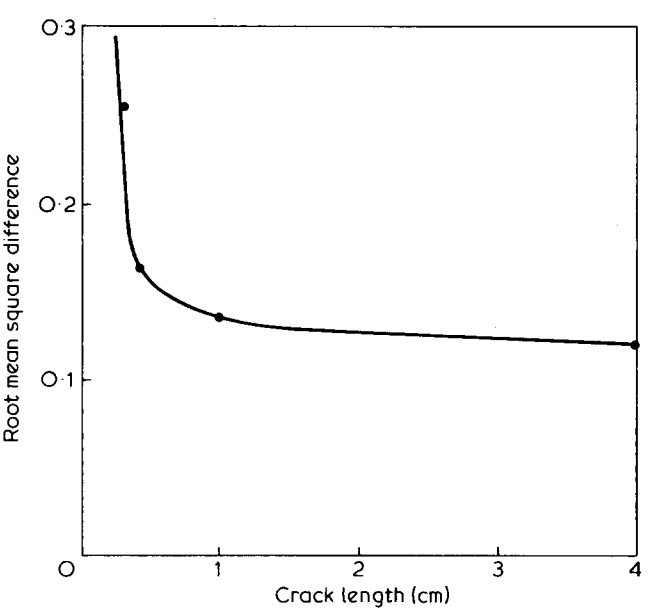

Figure 9 Variation of the root mean square deviation between observation and the model as a function of crack length

553 nm.) Using equation (6) gave the critical crack opening displacement δ_c equal to 4.20 μm.

From equation (2), when $x_1 = 0$ δ_c is given by

$$\delta_c = \frac{8\sigma_0 R}{\pi E^*} \quad (8)$$

Using $E^* = 2.95$ GPa (deduced from 4 point bend measurements and $\nu = 0.39$) and values for δ_c and R already stated, the craze stress σ_0 was found to be 112 MN m^{-2}. Finally, equation (5) was used to calculate the plane strain energy release rate $G_c = 0.47$ kJ m^{-2}. A summary of these results is shown in *Table 1*, which also shows how PES compares to similar work previously carried out on PMMA[4] and PC[2].

Similar tests were also carried out on the annealed material. Examples of the interference patterns produced are shown in *Figures 10a* and *b* and *11a* and *b*, for material annealed at 200°C for 1½ h and 5 h respectively. The loaded patterns are not in this case fully loaded due firstly to experimental constraints of loading the craze under the microscope, and secondly because it was not possible to resolve the individual fringes for the samples loaded beyond the points shown.

Table 1 Comparison of fracture parameters* between PES and other glassy polymers

	Measured *COD* δ (μm)	Measured craze length R (μm)	Craze stress σ_0 (MN m^{-2})	Plain strain strain energy release rate G_c (kJ m^{-2})
PMMA	2.2	29	83	0.182
PES	4.2 ± 0.1	43.5 ± 2	112 ± 14	0.47 ± 0.025
PC (lexan rod)	5.8	101	58	0.37

* Room temperature data (20°C)

There are two important differences between the craze shape and size brought about by annealing.

(i) The craze length R has been increased by annealing, the degree of lengthening being dependent on the annealing time as shown in *Figure 12*.

(ii) The overall shape has also been changed by annealing. A comparison between the unannealed and annealed materials is shown in *Figure 13a* an6 *b*. Note how the front portion of the treated craze has much straighter sides compared to the continuously curving shape of the Dugdale zone in the untreated material. Also note that on loading the extension at the rear of the craze is a larger percentage of the original displacement than the extension at the front of the craze, whereas in the untreated material the craze opens at a similar rate over its whole length.

On further extension it was noted that fringes continued to build up at the rear of the craze, eventually becoming unresolvable, while the fringe pattern in the front portion remained almost constant. This suggests that after annealing the craze stress is no longer constant over the whole length of the craze as is postulated by the Dugdale model, and therefore that the Dugdale equations can no longer be applied to calculate the fracture parameters δ_c, σ_0 and G_c. The difference between the experimental shape and the best fit to the Dugdale model is shown in *Figure 14*, using a similar method of fitting to that previously described. From this it is clear that for the annealed material the Dugdale plastic zone model no longer satisfactorily models the craze shape.

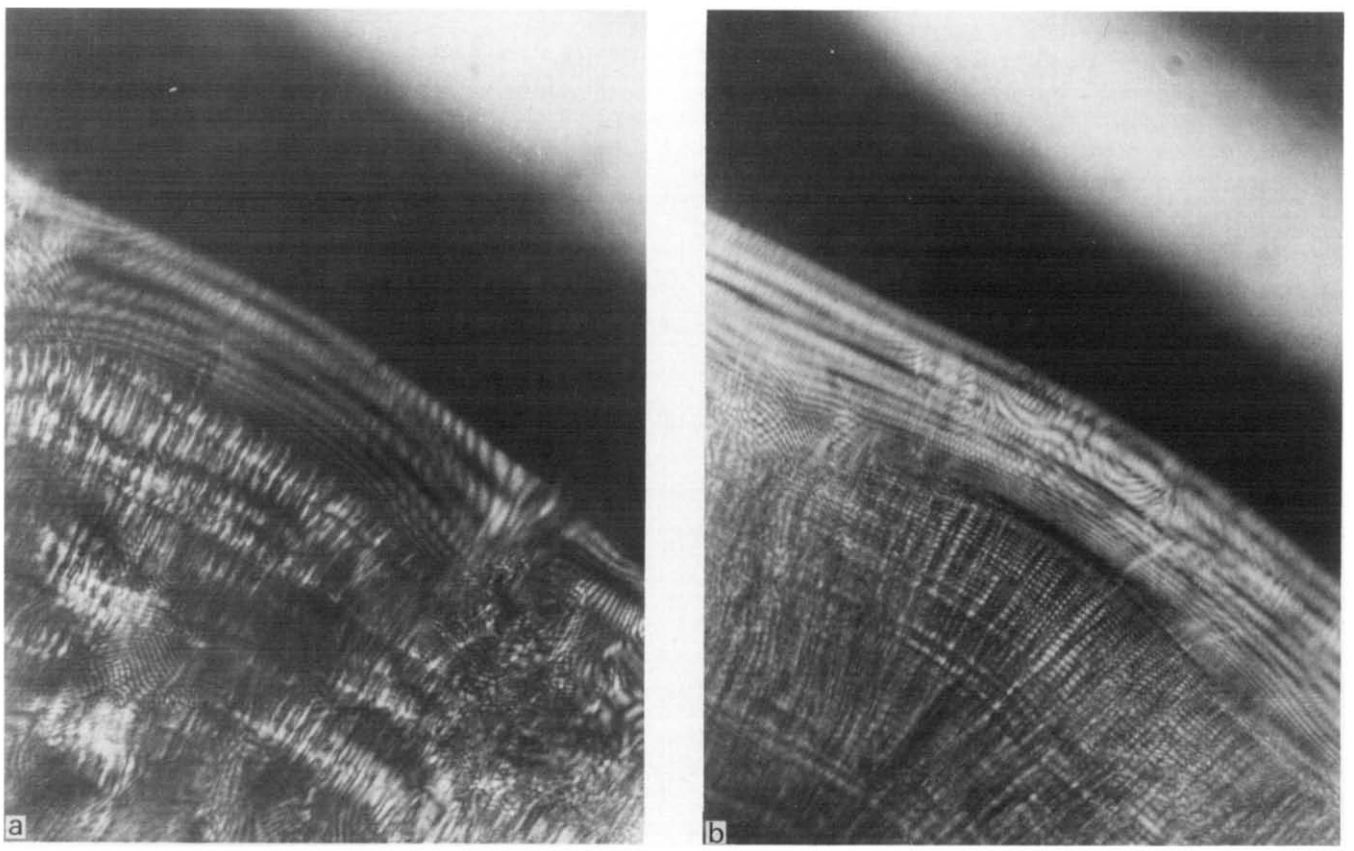

Figure 10 Interference patterns for material annealed at 200°C for 1½ hours (a) Unloaded and (b) Loaded

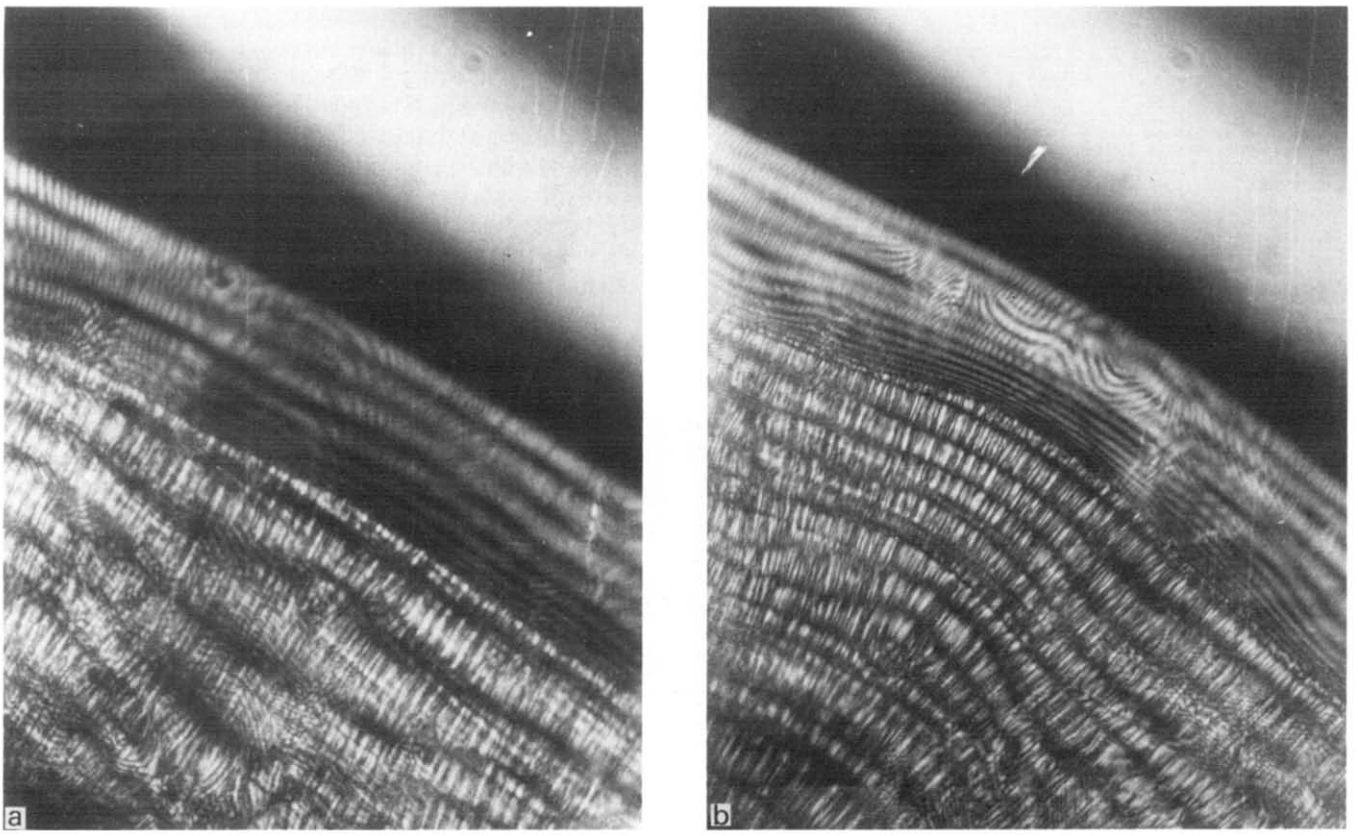

Figure 11 **Interference patterns for material annealed at 200°C for 5 hours (a) Unloaded and (b) Loaded**

Fracture toughness measurements

Fracture toughness tests were carried out as described above and a value for the critical strain energy release rate G_c was calculated for each sample tested using equation (1). The values obtained were much larger than those predicted by the Dugdale zone model, and following previous work this was attributed to the presence of sometimes large shear lips on the fracture surfaces. An example of such a region is shown in *Figure 15a* while *Figure 15b* shows the schematic representation of this form of failure which is similar to that seen in polycarbonate[1,2].

Two alternative models have been proposed to analyse this mixed mode failure in polymers. In the first of these Parvin and Williams[3] postulated (i) the existence of plane stress zones on each surface of the specimen of width equal to that of the plastic zone $r_p = \frac{1}{2\pi}(K_c/\sigma_y)^2$ (although they found them to be ten times smaller than expected), together with a central plane strain zone, (ii) that each region was characterised by its own critical K_c value and that the aggregate had properties which could be calculated from these individual values weighted proportional to the area of the fracture surface failing in each mode.

Fraser and Ward[1] and later Pitman and Ward[2] actually identified plane stress shear lips on the fracture surfaces of PC and measured the actual area involved in each failure mode. Pitman and Ward argued on physical grounds that the basic measurement was in terms of the energy of fracture and so proposed that the specimen was characterised by an apparent fracture toughness G_{cm} which was determined by the G_c values for the plane stress and plane strain regions weighted according to their area.

On the assumption that the energies required for craze propagation (plane strain) and ductile drawing in the shear lips (plane stress) are additive, we follow Pitman and Ward[2] in postulating that the combined strain energy release rate G_{cm} is given by

$$G_{cm} = G_{cps}\frac{B-w}{B} + \frac{\varphi}{2}\frac{w^2}{B} \tag{9}$$

where w = total shear lip width, B = sample thickness, φ is the energy to rupture per unit volume and G_{cps} is the plane strain critical strain energy release rate, which can be identified with that measured from the craze dimensions. Multiplying throughout by $B/(B-w)$ gives

$$G_{cm}\ \frac{B}{B-w} = G_{cps} + \frac{\varphi w^2}{2(B-w)} \tag{10}$$

In principle it is therefore possible to determine G_{cps} and φ from a plot of $G_{cm}B/(B-w)$ *versus* $w^2/(B-w)$ using data from a selection of samples with different shear lip widths. Results obtained in this investigation from the unannealed polymer, are shown in *Figure 16*. Although they show a substantial scatter these data, together with the value of G_{cps} measured independently from the craze shape analysis, lend considerable support to the form of mixed mode crack propagation as summarised in equations (9) and (10). The full line on the figure is a best fit through the data with intercept equal to the value of G_{cps} measured from the craze shape.

Further support for the mixed mode model is obtained by comparison of the value of φ measured from the slope of *Figure 16*, and the energy to rupture per unit volume

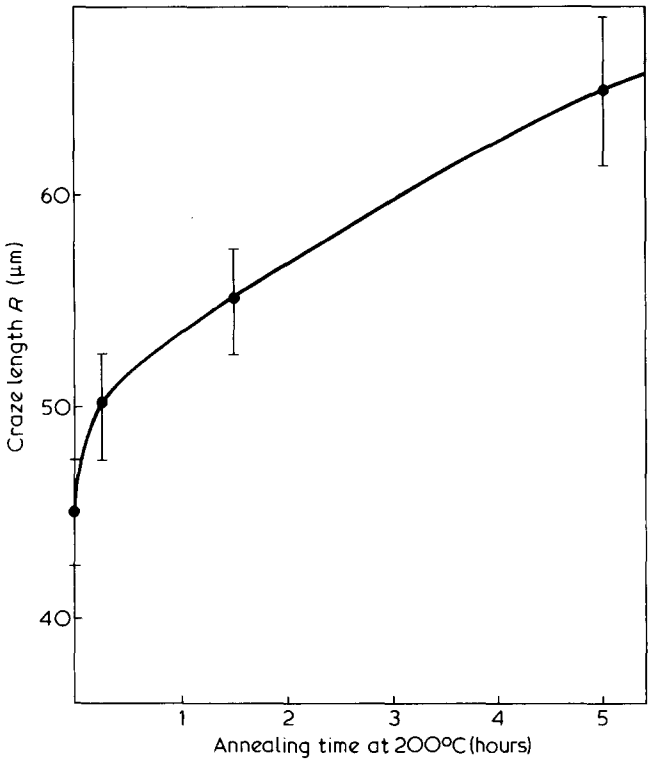

Figure 12 Variation of the craze length with annealing time

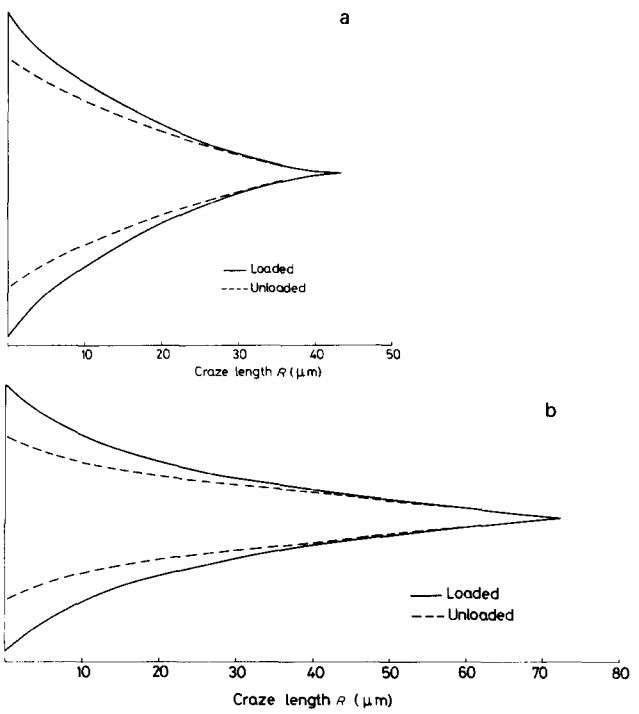

Figure 13 Comparison of the unloaded and loaded craze shape (a) Untreated material (b) Material annealed for 5 hours

measured directly from a simple unnotched tensile specimen. A typical load/displacement diagram for PES in a simple tension test is shown in *Figure 17*. The energy to yield unit volume of the material is proportional to the area under the curve, and was estimated to be 100 MJm^{-3} for a test at 0.05 cm min^{-1}. This value compares very favourably with the value of 80 MJm^{-3} obtained from the slope of *Figure 16*. The comparison is particularly good when one considers the difficulty in estimating the volume of yielded material in the shear lips.

The scatter in the data shown in *Figure 16* merits some discussion. Much of it derives from estimating the mean shear lip width for each sample. In many cases the shear lip width was far from constant and so the mean value was relatively inaccurate. Variations in shear lip width also resulted in fluctuations in load and crack velocity during crack propagation. It seems probable that instantaneous values of G_m would correlate better with the current shear lip width, but such a point by point correlation is not practicable.

Similar fracture tests were also carried out on the annealed materials. Shear lips were again in evidence on the surface, although becoming smaller as the annealing time increased. The data were plotted in the form of $G_{cm}B/(B-w)$ vs. $w^2/(B-w)$ in order to discover to what extent the plane strain and plane stress deformation modes were affected by annealing. Plots similar to *Figure 16* were obtained, differing only in that no independent measures of G_{cps} were available because the craze shapes for the annealed materials could not be accurately described by the Dugdale model. From the graphs however it was possible to estimate G_{cps} and φ from intercept and slope, and *Tables 2* and *3* show how these parameters vary with annealing time. These data, although subject to considerable uncertainties do indicate that (1) G_{cps} increases with annealing time, rapidly at first, and then levels off, (2) φ initially falls with annealing, largely due to a fall in extension to break (see *Table 3*). In addition it has been noted that the total shear lip width also decreases with increasing annealing time.

Based on these observations it is useful to consider the variation of overall strain-energy release rate G_{cm}. Referring to equation (9) it can be seen that the contribution from the first term increases with annealing time, both because of the rise in G_{cps} and also because of the decrease in shear lip width w. Conversely the contribution from the second term falls, due mainly to the decrease in the shear lip width.

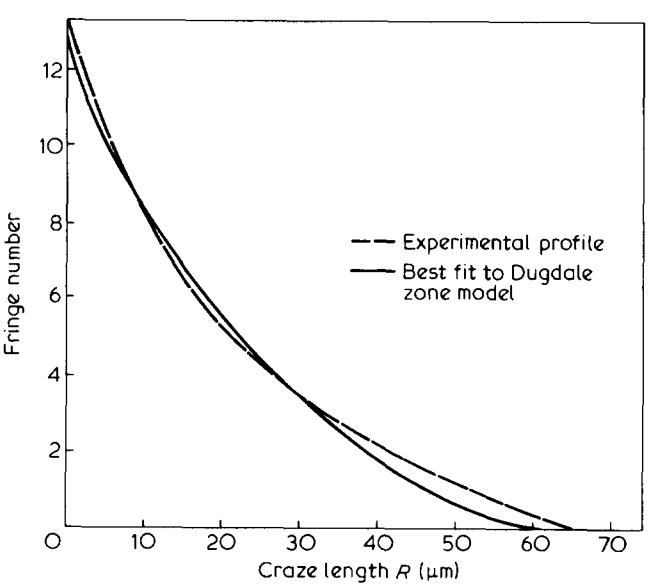

Figure 14 Comparison of experimental shape with the model for material annealed for 5 hours

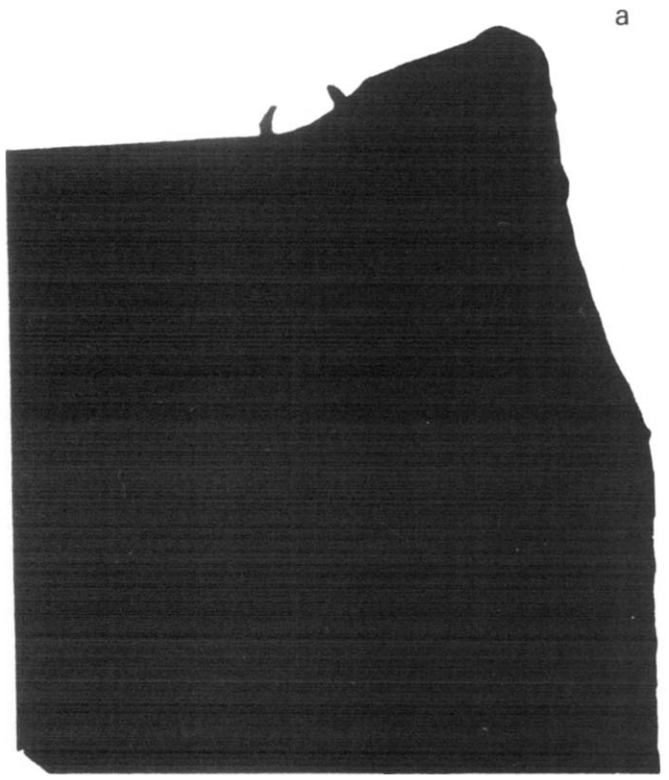

Figure 15 (a) Example of a shear lip (b) schematic representation of the mixed mode fracture model

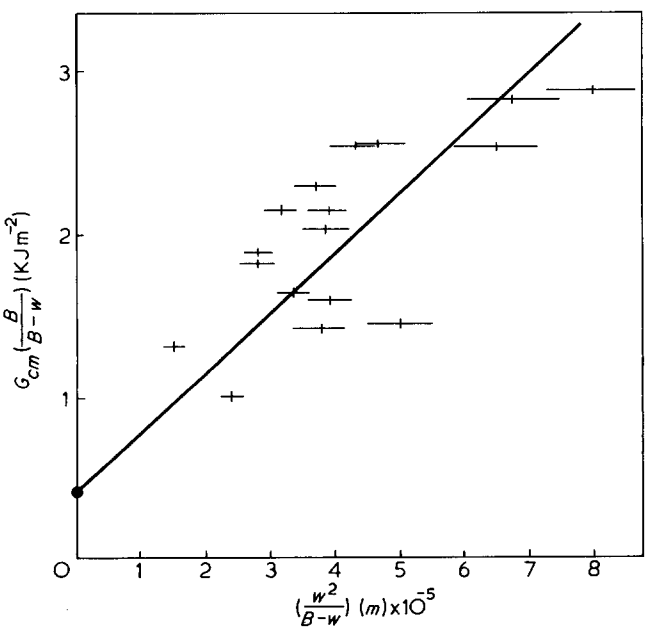

Figure 16 Mixed mode model plot for untreated PES

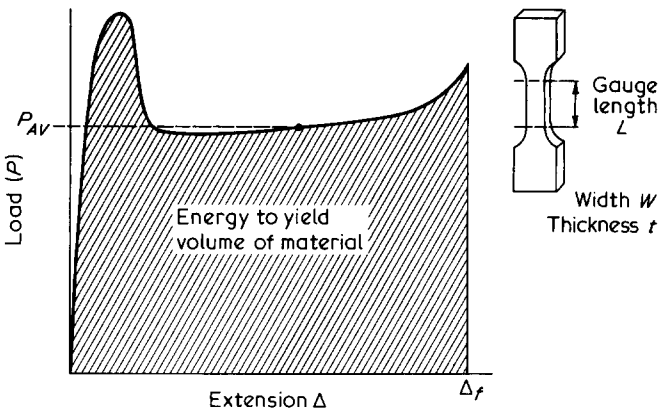

Figure 17 A typical load/displacement graph for PES in simple tension

Table 2 G_{cps} and ϕ^* obtained from the mixed mode model, for various annealing times

Annealing time (h)	Plane strain strain-energy release rate (kJ m^{-2})	Energy to break/unit volume (MJ m^{-3})
0	0.47 ± 5%**	80 ± 20%
1½	1.55 ± 20%	35 ± 20%
5	1.52 ± 15%	58 ± 20%

* Room temperature data following annealing at 200°C
** Value calculated from craze shape measurements

Table 3 Yield stress, extension to break and energy to yield obtained from tensile tests (temperature approx. 20°C, strain rate ~10^{-4} s^{-1})

Annealing time (h)	Yield stress (MN m^{-2})	Extension to break (For a 7.62 cm gauge length/cm)	Energy to break/ unit volume (MJ m^{-3})
0	85 ± 2%	1.49 ± 8%	115 ± 10%
3	96 ± 2%	0.45 ± 13%	36 ± 15%
6	98 ± 2%	0.79 ± 23%	61 ± 25%

It can be seen therefore that with this type of behaviour the variation of overall strain energy release rate G_{cm} could either rise or fall continuously on annealing, or show a maximum or minimum value depending on the relative magnitudes and rates of change of the relevant factors. For PES it was found that for the unannealed material the plane strain contribution (first term) was about a quarter of the plane stress contribution. On annealing the first term increased then levelled off, and the second term slowly decreased such that G_{cm} initially increased with annealing time and then began to fall.

The mixed mode model of fracture toughness is of considerable value in providing a framework to describe these relatively complex effects of annealing. It does not however provide any understanding either of the molecular changes occurring and how these result in the observed changes in the material parameters G_{cps} and φ, nor in particular, of the magnitude of the shear lip width w.

The shear lips develop on the surface where there is a situation of plane stress, and consist of material which has deformed under conditions very similar to that in a thin

sheet, essentially yielding and cold drawing to failure. In the central section of the sample, on the other hand, the state of stress corresponds to plane strain, and crazing occurs. In general terms the width of the shear lips will change as the relative magnitudes of the yield and craze stress change. Because the magnitude of the shear stress is of primary importance in determining yield whereas the hydrostatic component of stress plays a key role in crazing, a quantitative discussion would require a detailed analysis of the stress field at the tip of a crack with a craze and shear lips. In the absence of such an analysis the discussion must be of a qualitative nature. It can be concluded that if the yield stress increases at constant craze stress, the shear lips will decrease. It is found that the shear lips decreased on annealing, and also that the yield stress increases (*Table 3*). We can therefore conclude that the increase in yield stress is certainly greater than the increase in craze stress.

The indications from the mixed mode analysis are that G_{cps} increases markedly on annealing. Because the Dugdale zone modelling could not be applied to the annealing samples we do not have a direct measure of the craze stress from this source. However, it may be noted that the very large increase in G_{cps} on annealing is much larger than the increase in the yield stress. Taking into account the observed fall in the shear lips, it must therefore be concluded that the increase in G_{cps} is largely associated with an increase in crack opening displacement rather than an increase in the craze stress. Studies of the craze shape in annealed samples are continuing in attempt to define the situation more precisely.

CONCLUSIONS

(1) The mixed mode fracture model provides a satisfactory basis for understanding the fracture behaviour of polyethersulphone.

(2) For long cracks in unannealed samples the craze shape was in good agreement with that predicted by the Dugdale plastic zone model. Significant discrepancies between the observed shape and that predicted by this model were observed for short cracks in unannealed samples, and for cracks of all lengths in annealed samples.

(3) In general terms the fracture behaviour of polyethersulphone is intermediate between polycarbonate and polymethylmethacrylate. (The plane strain component of PES is actually higher than that of polycarbonate, but the shear lip widths are smaller, reducing the plane stress contribution, so that the overall toughness is lower).

(4) The effects of annealing are complex, in that the yield stress increases, the plane strain fracture toughness associated with the craze increases, and the shape of the craze changes markedly. It is still possible to gain qualitative understanding in terms of the mixed mode fracture model, but further studies are required if a quantitative treatment is to be obtained.

ACKNOWLEDGEMENTS

We are indebted to Dr D. Sims, Ministry of Defence,Procurement Executive, PERME for injection moulding the plaques. P. J. Hine was supported by a studentship from the Ministry of Defence.

REFERENCES

1 Fraser, R. A. W. and Ward, I. M. *Polymer* 1978, **19**, 220
2 Pitman, G. L. and Ward, I. M. *Polymer* 1979, **20**, 895
3 Parvin, M. and Williams, J. G. *J. Mater. Sci.* 1975, **10**, 1883
4 Brown, H. R. and Ward, I. M. *Polymer* 1973, **14**, 469
5 Döll, W. and Weidmann, G. W. *Colloid Polym. Sci.* 1976, **254**, 205
6 Vavakin, S. A., Kozyrev, Yu. I. and Salganik, R. Z. *Izrest. Akad. Nauk SSR, Mekh Tverd Tela* 1976, **11**, 111
7 Dugdale, D. S. *J. Mech. Phys. Solids* 1960, **8**, 100
8 Rice, J. R. in 'Fracture—An Advanced Treatise' (Ed. H. Liebowitz) Academic Press, New York and London, 1968, Chapter 3
9 Rice, J. R. *Proc. 1st Int. Conference on Fracture, Sendai, Japan*, 1966, **1**, 283
10 Wiley, R. H. and Brauer, G. M. *J. Polym. Sci.* 1948, **3**, 455 and 647
11 Morgan, G. P. and Ward, I. M. *Polymer* 1977, **18**, 87
12 Kambour, R. P. *Polymer* 1964, **5**, 143